



Increased ocular wall thickness and decreased globe volume in children with mucopolysaccharidosis type VI

Ozlem Ozkale Yavuz

Ercan Ayaz

Yilmaz Yıldız

Ayca Akgoz Karaosmanoglu

Elif Bulut

H. Serap Kalkanoglu Sivri

Kader K. Oguz

PURPOSE

Although clinical ophthalmologic findings have been reported, no study documented magnetic resonance imaging (MRI) findings in mucopolysaccharidosis (MPS) type VI. The aim of this study was to determine the ophthalmologic imaging findings of MPS type VI in the pediatric age group retrospectively.

METHODS

Brain MRIs of 10 patients with MPS type VI and 49 healthy children were evaluated independently by two pediatric radiologists for the following characteristics: globe volume, ocular wall thickness, and optic nerve sheath diameter for each orbit. The means of the measurement of each group were compared by using an independent t-test. Agreement and bias between reviewers were assessed by intra-class correlation coefficients (ICC).

RESULTS

A total of 59 children [32 girls (54.23%), 27 boys (45.77%); age range, 4-16 years; mean age, 10.37 ± 3.73 years] were included in the study. Statistical analysis revealed smaller eyeballs and thicker ocular walls of patients with MPS type VI ($P < .001$ and $P < .001$, respectively). However, there was no statistically significant difference in terms of optic nerve sheath diameter between the two groups ($P = .648$).

CONCLUSION

Patients with MPS type VI displayed reduced globe volumes and increased ocular wall thicknesses compared to the healthy children. Therefore, we recommend that ophthalmologic imaging findings might prove to be an auxiliary tool in the diagnosis of MPS patients.

The mucopolysaccharidoses (MPSs) are defined as a group of lysosomal storage diseases in which an inherited deficiency of one or more of the enzymes involved in the degradation of glycosaminoglycans (GAGs) occurs, leading to progressive GAG accumulation in organs and connective tissues of the body. Patients can have hearing impairment, skeletal deformities, cardiopulmonary disease, neurological, and intellectual and ophthalmological disorders.¹⁻³

Neuroradiologic and musculoskeletal findings of MPS have been well described in the radiology literature.¹⁻⁵ Ocular manifestations of MPS patients which include corneal clouding, ocular hypertension/glaucoma, retinal degeneration, optic disc swelling, and optic nerve atrophy have been also reported from clinical and/or ophthalmologic perspectives.⁶⁻⁸ To our knowledge, there is no well-documented comparative study regarding the ophthalmologic magnetic resonance imaging (MRI) findings of MPS type VI in children in the radiology literature. It is important to be familiar with the imaging findings of ophthalmologic abnormalities in MPS type VI patients in order to avoid diagnostic confusion.

In this study, we aimed to document ophthalmologic findings of MPS type VI which could be detected during evaluation of brain MRIs. We hypothesized that significant morphologic alterations occur in pediatric patients with MPS type VI as assessed by MRI.

Department of Radiology (O.O.Y. ✉ drozlemozkale@hotmail.com), Ankara Bilkent City Hospital, Ankara, Turkey; Department of Radiology (E.A.), Diyarbakir Children Hospital, Diyarbakir, Turkey; Division of Metabolism and Nutrition (Y.Y., H.S.K.S.), Department of Pediatrics, Hacettepe University School of Medicine, Ankara, Turkey; and Department of Radiology (A.A.K., E.B., K.K.O.), Hacettepe University School of Medicine, Ankara, Turkey.

Received 1 April 2021; revision requested 18 June 2021; last revision received 22 October 2021; accepted 3 November 2021.

Publication date: 5 October 2022.

DOI: 10.5152/dir.2022.21372

You may cite this article as: Yavuz OO, Ayaz E, Yıldız Y, et al. Increased ocular wall thickness and decreased globe volume in children with mucopolysaccharidosis type VI. *Diagn Interv Radiol.* 2022;28(5):516-521.

Methods

Patients

This study received institutional review board approval from our university ethical committee with a protocol number of GO 21/275, and the informed consent was waived. It took a 2-month period from June through August 2019 for analysis of the brain MRIs of patients under 18 years of age. The archives in the database of neuroradiology and division of the pediatric metabolism were used for recruiting subjects in the study. Ten children diagnosed with MPS type VI and 49 otherwise healthy children who underwent brain MRI due to nonspecific complaints such as headache were evaluated. The inclusion criteria for children in the control group were being in the similar age range with the MPS type VI patients and having scans interpreted as normal brain and ophthalmologic findings in brain MRI as well as normal physical examination findings. Exclusion criteria for the study included motion artifacts, previous invasive cranial procedures, cranial deformity, and patient history of orbital or optical impairment.

Clinical and demographic information regarding the MPS patients, including the age at diagnosis and also at initiation of enzyme replacement therapy, organ involvement, and causative arylsulfatase B (*ARSB*) gene mutations, were retrieved retrospectively from hospital records. Findings of the ophthalmological examinations temporally closest to the acquisition of the brain MRI were also noted.

MRI protocol and image analysis

Finally, brain MRIs of 10 patients with MPS type VI and 49 healthy children were evaluated independently by two pediatric radiologists for the following

characteristics: globe volumes, ocular wall thicknesses, and optic nerve sheath diameters for each orbit. All MRI studies had been performed using 1.5T scanners (Symphony (Siemens) and Achieva (Philips)) and included routine brain protocol sequences in all pediatric patients. Axial T2-weighted (W) images (WI) (repetition time, 3000 ms; echo time, 100 ms; field of view, 240 mm; matrix, 256 × 256) obtained with 4 mm slice thickness and 10% interslice gaps were used for all measurements. Axial sections were used because they are reproducible and are acquired according to a well-defined standard view. In addition, axial images are routinely used in any basic examination and thus are most likely imaging series to be available for the reviewing radiologist. The measurements were performed using Syngo via (VB10, Siemens AG) on a workstation. The circumferential area of the globe, including the walls of the globe, was manually outlined in all axial contiguous sections of T2W images, and the volume of each globe was calculated semi-automatically (Figure 1). It is not possible to distinguish 3 primary layers: the sclera (outer), uvea (middle), and retina (inner layer) of the ocular wall on brain MRI. Therefore, the thickness of all sclera-choroid-retinal layers was considered as ocular wall thickness. Maximum thickness of ocular wall complex was also measured for each eye. The optic nerve sheath was measured diametrically from 10 mm anterior to the optic foramen on each side (Figure 1).

Statistical analysis

Data analysis was performed by IBM SPSS Statistics 25.0 software package (IBM Corp.). We assessed mean ± standard deviation (SD) of globe volumes, ocular wall thicknesses, and optic nerve sheath diameters for both patient group and control group. Statistical significance level was taken as $P=0.05$. Descriptive statistics of the data were presented with n (%). The evaluation of gender difference between patient group and control group was assessed using Fisher exact test. Normalized distributions were shown as mean ± SD. Kolmogorov–Smirnov test was used as test of normality for each measurement. The means of the measurement of each group were compared by using an independent sample t-test. Agreement and bias between reviewers were assessed by intra-class correlation coefficients (ICC). Agreement based on ICCs was interpreted

as follows: 0-0.39=poor, 0.40-0.59=fair, 0.60-0.74=good, and 0.75-1.0=excellent.⁹ Pearson correlation coefficient has been calculated to evaluate correlation of globe volume changes by age of the two groups (healthy and MPS type VI patients).

Results

A total of 59 children were included in this study. Thirty-two of 59 children (54.23%) were female and 27 of 59 children (45.77%) were male. Their age ranged from 4 years to 16 years (mean age: 10.37 ± 3.73 years). Five of 10 children with MPS type VI (50%) were female and 5 of 10 children (50%) were male. Their age ranged from 4 years to 15 years (mean age: 10.40 ± 3.84 years). Twenty-seven of 49 healthy children (55.10%) were female and 22 of 49 healthy children (44.90%) were male. Their age ranged from 4 years to 16 years (mean age: 10.37 ± 3.72 years). The mean age and gender did not differ significantly between both MPS type VI and healthy group ($P=.911$ and $P=1.000$, respectively).

Clinical characteristics of the patients with MPS type VI are presented in Table 1. The age at diagnosis ranged from 12 months to 12 years. All patients had the rapidly progressive form of MPS type VI and had various degrees of corneal involvement near the time of brain MRI, some with additional ophthalmological findings as depicted in Table 1. One patient (patient no. 1) had bilateral vision loss, attributed to severe opacification of the cornea due to GAG deposits. Another patient (patient no. 7) had papilledema due to hydrocephalus. The diameter of optic sheath-nerve complex was 0.57 cm for right globe, 0.47 cm for left globe, and the mean diameter was 0.52 cm. This measurement was the same as the mean value of optic sheath-nerve diameter of MPS type VI patients and was close to the values of healthy children. Clinically discernible abnormalities regarding the size of the globes were not mentioned in the medical charts.

All patients had normal vitreous signal intensity, and none had a hemorrhage or focal lesion in the globe on visual evaluation of MRI. Globe volumes, ocular wall thicknesses, and optic nerve sheath diameters of MPS type VI patients and healthy group were normally distributed according to Kolmogorov–Smirnov test (both, $P>.05$). Mean ± SD of globe volumes, ocular wall thicknesses, and optic nerve sheath

Main points

- Substantial morphologic changes occur in pediatric patients with mucopolysaccharidosis (MPS) type VI as assessed by magnetic resonance imaging.
- The mean globe volumes of patients with MPS type VI were statistically smaller, and the ocular walls of patients with MPS type VI were statistically thicker than those of healthy control subjects.
- Ophthalmologic imaging findings may be one of the tools to aid in the diagnosis of MPS disease.

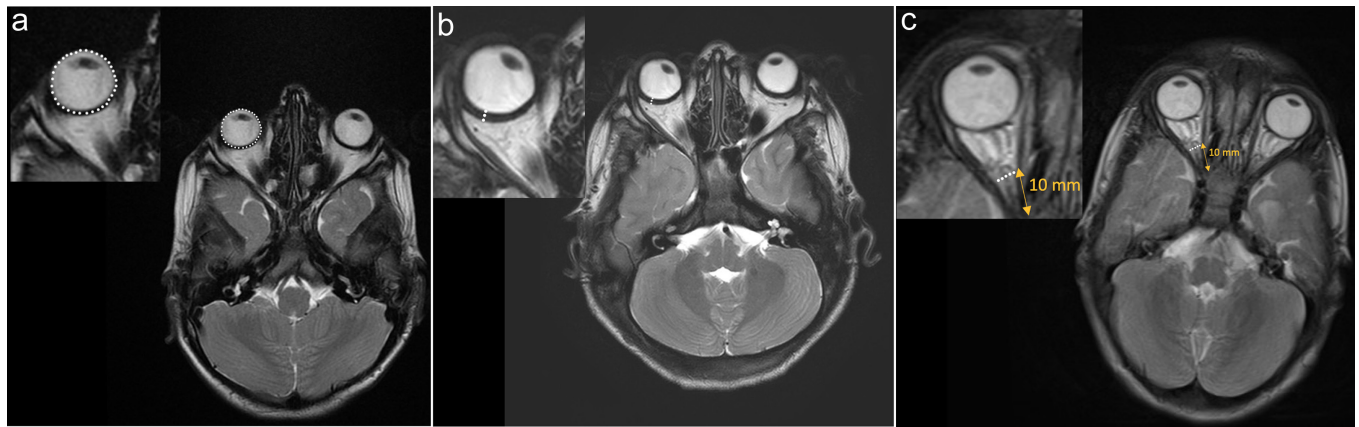


Figure 1. A 6-year-old boy with MPS type VI. Axial T2-weighted (W) brain MRI shows manual outlining of the right globe for volume measurement (a). A 12-year-old boy with MPS type VI. Axial T2-weighted brain MRI reveals measurement of ocular walls composing sclera-choroid-retinal layers which seem thick bilaterally (b). T2W image of another girl with MPS type VI at 5 years of age shows measurement method of optic nerve sheath diameter at 10 mm anterior to the optic foramen. In this patient, a distended nerve sheath is seen (c). MPS, mucopolysaccharidose; MRI, magnetic resonance imaging.

diameters of MPS type VI and healthy children are presented in Table 2. The mean \pm SD of globe volumes determined in healthy

group and children with MPS type VI were $13.18 \pm 1.89 \text{ cm}^3$ and $11.26 \pm 1.36 \text{ cm}^3$, respectively. The mean \pm SD of ocular wall

thicknesses detected in healthy group was $0.14 \pm 0.04 \text{ cm}$ and was $0.18 \pm 0.07 \text{ cm}$ in children with MPS type VI. Patients with

Table 1. Demographic characteristics, clinical features and ophthalmologic examinations of patients with MPS type VI

Patient number	Sex	Age at diagnosis	Age at starting ERT	Clinical features ^a	Ophthalmologic examination (age)	ARSB gene mutations ^b
1	F	4 years	6 years	Macrocephaly, valvulopathy, ventricular hypertrophy, chronic otitis media with effusion, hernias	Corneal clouding with dense stromal deposits, exophthalmos, optic disc pallor, nystagmus, no visual fixation (14 years)	c.962T>C (p.Leu321Pro)
2	F	21 months	2.5 years	Mild valvulopathy, obstructive sleep apnea	Corneal clouding, glaucoma (12 years)	c.962T>C (p.Leu321Pro)
3	M	3 years	11 years	Macrocephaly, obstructive sleep apnea, chronic respiratory failure, tracheostomy, valvulopathy, severe cervical cord compression, hernias	Corneal stromal clouding, mild exophthalmos, increased retinal vascular tortuosity, palpebral deposits (14 years)	c.1036delG (p.Leu346Serfs*11)
4	M	2 years	6 years	Cardiac hypertrophy, severe valvulopathy and aortic root dilatation, severe cervical cord compression, hernias, chronic otitis media with effusion	Corneal clouding myopia, conjunctival injection (12 years)	c.962T>C (p.Leu321Pro)
5	M	12 years	12 years	Mild valvulopathy	Mild corneal edema (12 years)	c.1168G>A (p.Glu390Lys)
6	M	12 months	4 years	Macrocephaly, chronic otitis media with effusion, hernias, mild valvulopathy, severe cervical cord compression	Corneal clouding (8 years)	c.962T>C (p.Leu321Pro)
7	F	4 years	4 years	Macrocephaly, hydrocephalus, severe valvulopathy, heart failure, obstructive sleep apnea, pulmonary hypertension	Papilledema ^c , corneal stromal deposits, strabismus (4 years)	c.962T>C (p.Leu321Pro)
8	M	12 months	15 months	Valvulopathy, chronic otitis media with effusion, hernias	Mild corneal clouding (4 years)	c.962T>C (p.Leu321Pro)
9	F	5 years	6 years	Chronic otitis media with effusion, moderate valvulopathy	Corneal clouding (11 years)	c.962T>C (p.Leu321Pro)
10	F	4 years	4 years	Valvulopathy, heart failure	Diffuse corneal clouding, a single retinal drusen (9 years)	c.962T>C (p.Leu321Pro)

^aShort stature, skeletal deformities, and dysmorphic facial features are clinical features common to all listed patients. Additional clinical findings are depicted in the table.

^bAll patients are homozygous for the listed mutations.

^cResolved after correction of hydrocephalus.

MPS, mucopolysaccharidose; ERT, enzyme replacement therapy.

Table 2. Mean \pm standard deviation and *P*-values of globe volumes, ocular wall (sclera-choroidea-retina) thickness, and optic nerve sheath diameter of MPS type VI and healthy children

	Mean \pm SD	<i>P</i> *
Globe volume (cm ³) (MPS type VI)	11.26 \pm 1.36	<.001
Globe volume (cm ³) (healthy group)	13.18 \pm 1.89	
Ocular wall thickness (cm) (MPS type VI)	0.18 \pm 0.07	<.001
Ocular wall thickness (cm) (healthy group)	0.14 \pm 0.04	
Optic nerve sheath diameter (cm) (MPS type VI)	0.52 \pm 0.10	.648
Optic nerve sheath diameter (cm) (healthy group)	0.51 \pm 0.07	

* independent samples t-test.
SD, standard deviation; MPS, mucopolysaccharidosis.

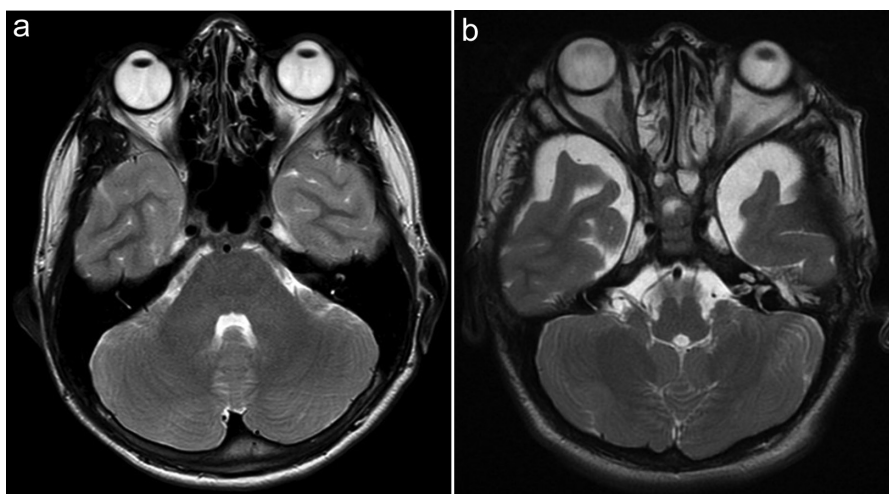


Figure 2. A 12-year-old healthy boy (a) and 12-year-old boy with MPS type VI (b). Note the smaller globes and thicker ocular wall layers in the patient compared with the age- and sex-matched healthy control subject.

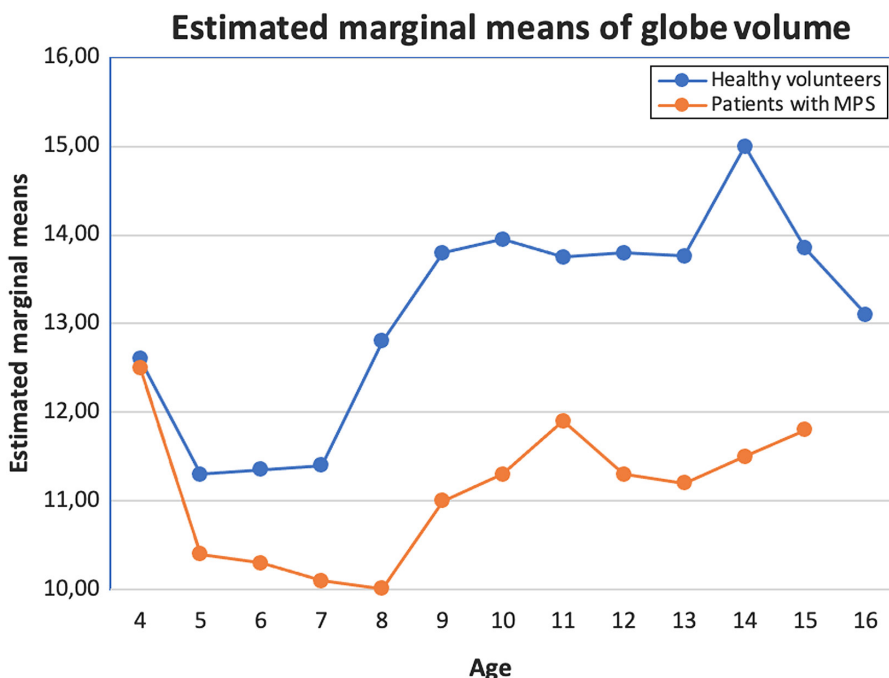


Figure 3. Estimated mean values of globe volumes of children with MPS and healthy control groups according to age.

MPS type VI had significantly smaller mean globe volumes and greater ocular wall thicknesses than the healthy children ($P < .001$ and $P < .001$, respectively) (Figure 2). On the other hand, the mean \pm SD of optic nerve sheath diameters reported in healthy group and children with MPS type VI were 0.51 \pm 0.07 cm and 0.52 \pm 0.10 cm, respectively. Optic nerve sheath diameters did not differ between the 2 groups ($P = .648$). Agreement between reviewers was fair for globe volume (ICC: 0.554, $P < .001$), fair for sclera-choroidea-retina thickness (ICC: 0.531, $P < .001$), and weak for optic nerve sheath diameter (ICC: 0.327, $P < .001$).

The estimated mean values of globe volume by age of patients with MPS and healthy volunteers are shown in Figure 3. For determining correlation of globe volume changes by age, Pearson correlation coefficient for healthy children and study cohort was 0.366 ($P < .001$) and 0.309 ($P < .001$), respectively.

Discussion

The most important finding of this study was that the patients with MPS type VI had smaller globe volumes and thicker ocular wall layers compared to the healthy children. To the best of our knowledge, our study is the first study which presents the ophthalmologic imaging abnormalities of MPS type VI on MRI in the pediatric population. These findings may serve as an auxiliary criterion in routine clinical evaluation of MPS.

MPS type VI also known as Maroteaux-Lamy syndrome is inherited in an autosomal recessive pattern. MPS type VI is caused by deficiency of arylsulfatase B (N-acetylglucosaminidase-4-sulfatase), leading to deposition of dermatan sulfate. The signs of MPS type VI include coarse facial features, umbilical hernia, skeletal deformities (e.g., dysostosis multiplex), restriction of joint movement, cardiac valvular abnormalities, hepatosplenomegaly, and macroglossia. Patients may also present with hydrocephalus and spinal stenosis.

Ocular pathology is also common in patients with MPS, since the eye as well as other tissues accumulate excessive amounts of GAGs. The widespread GAG accumulation in entire ocular tissue leads to a vast array of ocular manifestations. In the literature, there are many articles describing the typical ocular features

which include corneal clouding, ocular hypertension/glaucoma, retinal degeneration, and optic nerve atrophy mainly by ophthalmologists.^{6,7,10,11} GAG deposition within retinal pigment epithelial cells and in the photoreceptor matrix leads to progressive photoreceptor loss, retinal degeneration, and dysfunction of the remaining photoreceptors.⁸ Predominantly, retinal degeneration in patients with MPS type I, MPS type II, MPS type III, and MPS type IV are reported.^{6,8} In our study, corneal clouding due to stromal deposits was observed in 80% of patients with MPS type VI, and it was the most common ophthalmologic finding. In addition, 20% of patients with MPS type VI had alterations in retinal layers. Schumacher et al.¹² documented his experience in a total of 65 patients with MPS (18 type I, 12 type II, and 35 type VI) and healthy volunteers. Similar to our findings, they demonstrated thickening of the sclera MPS type I, II, and VI patients using ultrasound examination. However, increased optic nerve sheath thickness was also revealed in that study. GAG deposition causes thickening of the sclera with consequent compression of the optic nerve resulting in optic disk swelling and subsequent optic nerve atrophy in cases with prolonged compression.^{10,13} There are also many articles that mentioned corneal thickening and increased corneal rigidity as a reason for glaucoma in patients with MPS.^{10,14,15} In histopathological examination, normal sclera thickness is 1 mm around the optic disc and 0.6 mm at the equator. The thickness of the retina is 0.1 mm at the fovea centralis and 0.56 mm near the optic disc.^{16,17} Using MRI, we cannot distinguish the individual layers of the outer lining of the eyeball. They appear as a homogeneous hypointense band-like structure on T2W images. MRI findings in the current study support the literature reporting thicker ocular wall layers of the globe on ophthalmologic examination in patients with MPS type VI. The maximum total thickness of the ocular wall in healthy children was 1.3-1.5 mm, and it was measured accordance to the sum of single layers determined by histological measurements. The morphologic changes seen in the globes of MPS type VI patients could be due to the accumulation of GAGs in the ocular wall layers and consequent impairment of normal development.

Patients with Maroteaux-Lamy syndrome may have optic atrophy and

swelling or papilledema associated with hydrocephalus.⁶ In our study, optic sheath-nerve complex measurements did not differ significantly between each group. None but one of our patients had hydrocephalus, and in that particular patient, the optic sheath-nerve complex was almost the same to the mean values of the healthy group (0.52 mm vs. 0.51, respectively). Thus, a different group with more patients with hydrocephalus would yield significantly increased optic sheath-nerve complex. On the other hand, this could be due to the limitation of thicker slices (4 mm) of brain MRIs.

Studies have disclosed that age and gender affect ocular globe volume.¹⁸⁻²⁰ Furthermore, some studies have shown that any structures of the anterior or posterior eye segments such as the lens, retina, choroid, and primary vitreous affect the secondary vitreous enlargement by producing regulatory growth factors. Expansion of the secondary vitreous influences ocular growth. In some diseases such as retinal dysplasia, insufficient production of the secondary vitreous causes microphthalmia.^{21,22} In the current study, there were no differences in the mean age and gender between both MPS type VI and the healthy group. Similar to the literature, globe volumes increased by age in both groups in our study. However, GAG accumulation may have caused smaller ocular globe volumes by thickening and degeneration in the retinal, choroidal, or scleral layers. Moreover, ocular wall thickening in the dorsal region of the eyeball may lead to alterations in the shape of the eyeball in children with MPS. As we have a small study group, further studies with more patients and healthy volunteers are needed to evaluate age-related changes in globe volume.

Our study has several limitations. First, it is a retrospective study, and although we present ophthalmologic imaging features of specifically MPS type VI, the number of patients is still low due to its rarity. Second, the measurements were performed using brain MRIs. Because of well-defined physical ophthalmologic findings, usually ophthalmologists do not order orbit MRI in these patients. Thus, our examination was limited to the images with 4 mm slice thickness on brain MRIs and such submillimeter differences can be difficult to detect in routine brain MRI. Nonetheless, radiologists should be familiar with smaller globes with thicker walls in patients with MPS type VI

while reading cases to avoid unnecessary diagnostic tests.

In conclusion, ocular abnormalities in MPS type VI often lead to visual impairment. Our MRI findings of smaller globe volumes and thicker ocular wall layers can be used as an auxiliary noninvasive tool in the investigation of suspected children, and radiologists' awareness is important to avoid unnecessary diagnostic tests in these patients. Therefore, radiologists particularly should make a point of the routine evaluation of eye globe, while assessing brain MRI in MPS type VI patients.

Acknowledgments

The authors would like to thank the patients and their families and also acknowledge all the physicians and health care professionals who were involved in the diagnosis, management and follow-up of the patients included in this study.

Conflict of interest disclosure

The authors declared no conflicts of interest.

References

1. Rasalkar DD, Chu WCW, Hui J, Chu CM, Paunipagar BK, Li CK. Pictorial review of mucopolysaccharidosis with emphasis on MRI features of brain and spine. *Br J Radiol*. 2011;84(1001):469-477. [\[CrossRef\]](#)
2. Reichert R, Campos LG, Vairo F, et al. Neuroimaging findings in patients with mucopolysaccharidosis: what you really need to know. *RadioGraphics*. 2016;36(5):1448-1462. [\[CrossRef\]](#)
3. Nicolas-Jilwan M, AlSayed M. Mucopolysaccharidoses: overview of neuroimaging manifestations. *Pediatr Radiol*. 2018;48(10):1503-1520. [\[CrossRef\]](#)
4. Lachman R, Martin KW, Castro S, Basto MA, Adams A, Teles EL. Radiologic and neuroradiologic findings in the mucopolysaccharidoses. *J Pediatr Rehabil Med*. 2010;3(2):109-118. [\[CrossRef\]](#)
5. Shimoda-Matsubayashi S, Kuru Y, Sumie H, et al. MRI findings in the mild type of mucopolysaccharidosis II (Hunter's syndrome). *Neuroradiology*. 1990;32(4):328-330. [\[CrossRef\]](#)
6. Ashworth JL, Biswas S, Wraith E, Lloyd IC. Mucopolysaccharidoses and the eye. *Surv Ophthalmol*. 2006;51(1):1-17. [\[CrossRef\]](#)
7. Naik VD, Usgaonkar UPS, Albal VH. Retinal changes in mucopolysaccharidosis I- A case report. *Int J Ocul Oncol Oculoplasty*. 2018;4:67-72.
8. Ashworth JL, Biswas S, Wraith E, Lloyd IC. The ocular features of the mucopolysaccharidoses. *Eye (Lond)*. 2006;20(5):553-563. [\[CrossRef\]](#)
9. Hallgren KA. Computing inter-rater reliability for observational data: an overview and tutorial. *Tutor Quant Methods Psychol*. 2012;8(1):23-34. [\[CrossRef\]](#)

10. Ferrari S, Ponzin D, Ashworth JL, et al. Diagnosis and management of ophthalmological features in patients with mucopolysaccharidosis. *Br J Ophthalmol.* 2011;95(5):613-619. [\[CrossRef\]](#)
11. Kenyon KR. Ocular manifestations and pathology of systemic mucopolysaccharidoses. *Birth Defects Orig Artic Ser.* 1976;12(3):133-153.
12. Schumacher RG, Brzezinska R, Schulze-Frenking G, Pitz S. Sonographic ocular findings in patients with mucopolysaccharidoses I, II and VI. *Pediatr Radiol.* 2008;38(5):543-550. [\[CrossRef\]](#)
13. Collins ML, Traboulsi EI, Maumenee IH. Optic nerve head swelling and optic atrophy in the systemic mucopolysaccharidoses. *Ophthalmology.* 1990;97(11):1445-1449. [\[CrossRef\]](#)
14. Connell P, McCreery K, Doyle A, Darcy F, O'Meara A, Brosnahan D. Central corneal thickness and its relationship to intraocular pressure in mucopolysaccharidosis-1 following bone marrow transplantation. *J AAPOS.* 2008;12(1):7-10. [\[CrossRef\]](#)
15. Tonnu PA, Ho T, Newson T, et al. The influence of central corneal thickness and age on intraocular pressure measured by pneumotonometry, non-contact tonometry, the Tono-Pen XL, and Goldmann applanation tonometry. *Br J Ophthalmol.* 2005;89(7):851-854. [\[CrossRef\]](#)
16. Berry MM, Standring SM, Bannister LH. Nervous system. In: Williams PL, ed. *Gray's Anatomy.* 38th ed. New York: Churchill Livingstone; 1995:1322.
17. Funke RH, Appel DJ, Naumann GO. Embryologie, anatomie und Untersuchungstechnik. In: Doerr W, Seifert G, Uehlinger E, eds. *Spezielle pathologische Anatomie: Pathologie des Auges I.* Berlin: Springer; 1997:1-93.
18. Hahn FJ, Chu WK. Ocular volume measured by CT scans. *Neuroradiology.* 1984;26(6):419-420. [\[CrossRef\]](#)
19. Brémond-Gignac D, Cussenot O, Deplus S, et al. Computation of eyeball growth by magnetic resonance imaging (26.11.93). *Surg Radiol Anat.* 1994;16(1):113-115. [\[CrossRef\]](#)
20. Fledelius HC, Christensen AC. Reappraisal of the human ocular growth curve in fetal life, infancy, and early childhood. *Br J Ophthalmol.* 1996;80(10):918-921. [\[CrossRef\]](#)
21. Weiss AH, Kousseff BG, Ross EA, Longbottom J. Complex microphthalmos. *Arch Ophthalmol.* 1989;107(11):1619-1624. [\[CrossRef\]](#)
22. Newsome DA, Linsenmayer TF, Trelstad RL. Vitreous body collagen: evidence for a dual origin from the neural retina and hyalocytes. *J Cell Biol.* 1976;71(1):59-67. [\[CrossRef\]](#)